[redacted]

C.7

WAVE CHARACTERISTICS OF THE LIQUID LAYER IN HORIZONTAL ANNULAR FLOW

S.V. Paras and A.J. Karabelas

Chemical Process Engineering Research Institute and
Department of Chemical Engineering, University of Thessaloniki,
GR 540 06 Thessaloniki, Greece

1. INTRODUCTION

Reliable information on gas/liquid interface characteristics is extremely useful in understanding and modeling various aspects of annular flow, such as liquid atomization, friction losses and mass transfer. Experimental data on film wave characteristics in horizontal annular flow are very limited. The study of Sekoguchi et al (1982), in a 25 mm ID pipe, appears to be the only work where statistical liquid film characteristics are reported. Laurinat (1982) presents useful time-averaged film properties, in a 50 mm I.D. pipe, but no statistical analysis of the time records.

This publication is based on recently made detailed film thickness measurements, at various locations in the pipe circumference. Analysis of these data allows the determination of wave characteristics, such as RMS values, wave frequencies and celerities, as well as height, length, width and intermittency of large disturbance waves. It is expected that these quantities, complemented with other types of measurements, will place modeling of horizontal annular flow on a more sound basis.

2. FILM THICKNESS MEASUREMENTS

2.1 Flow Loop

For the purpose of this investigation a horizontal two-phase flow loop was designed and constructed. The pipeline consists of a 16 m long, 5 cm ID, straight pipe section and a 180° 5 cm ID bend, followed by a 8 cm ID pipe having a length of 16 m. The 5 cm pipe consists of two parts, a 9 m stainless steel part and a 7 m transparent plexiglas part to facilitate visual observations. The mixing section for the two phases is a simple tee with the liquid phase introduced in the branch and the gas phase in the run. The distance between the mixing section and the test-section is ≈15 m, i.e. approximately 300 pipe diameters. Details on the two phase flow loop are presented elsewhere (Paras and Karabelas, 1990).

2.2 Experimental Techniques

Wave heights and liquid film thickness along the pipe in two-phase flow are measured using parallel wire conductance probes. This measuring technique relies on the fact that the conductance between two parallel wires is uniquely related to the liquid level between them. The parallel wire probes require an electronic analyzer circuit (Andritsos, 1986), which measures

Paper presented at ICHMT Seminar on "Phase-Interface Phenomena in Multiphase Flow", May 14-18, Dubrovnik, Yugoslavia.

the conductance of the liquid film between the wires and produces a DC output corresponding to the film height.

A plexiglas test section was designed and constructed for film thickness measurements. The probes were in the form of plugs which could be inserted into the test section. The lower part of the plugs was machined so that they were flush with the inside pipe wall when mounted onto the test section. A total of 8 probes, spaced at 45° intervals, could be placed around the circumference of the pipe. The probes were chromel wires 0.5 mm in diameter, 10 mm long and 2.5 mm apart. A second set of 8 plugs could be located 6 cm upstream of the first set, holding similar conductance probes for performing cross-correlation film thickness measurements. Details on the probe accuracy and the calibration procedure are reported by Karapantsios et al (1989).

Three probes were fabricated with the intention to use them simultaneously. However, in preliminary tests an interaction of the electric fields of two neighboring probes was noticed, resulting in a reduction of the signal. Therefore, only one probe at a time was used to obtain film thickness data. Two- and three-probe measurements were performed simultaneously only in cases where qualitative results were required, e.g. for cross-correlation and comparison of film traces.

Measurements were taken at six circumferential positions, i.e. at the bottom (0°), at 45°, 90°, 135°, 180° and 315° from the bottom of the pipe. Originally the three probes were located at 0°, 90°, 180°. Rotating the test section by 45°, the probes were placed at 45°, 135° and 315° respectively. The range of superficial velocities covered in the tests, was U_L= 1.9 to 20 cm/s for water and U_G= 31 to 66 m/s for air, which corresponds to annular two phase flow.

2.3 Methods of Data Acquisition and Analysis

Analog signals from film thickness analyzers are converted to digital signals and are stored for subsequent analysis. Analog to digital conversion is performed by a 12-bit, 16-channel A/D converter and data obtained are transferred to a Macintosh Plus (1Mb) microcomputer for storage and analysis.

Each data set was collected for a period of 16.5 sec with a sampling frequency of 250 Hz. Data for wave celerity calculations were sampled for 1.5 sec with a sampling frequency of 1000 Hz.

Mean film thickness, RMS values of the film height fluctuations, spectral density function and cross correlation function are obtained from each data record by using time series analysis. Special software was developed for the analysis of the above quantities which are defined as in Bendot and Piersol (1971).

3. DATA ANALYSIS AND INTERPRETATION

3.1 Film Thickness and RMS Circumferential Distribution.

Representative data points, showing the film thickness distribution around the pipe circumference, are presented in Figure 1. Solid lines are interpolating curves, which fit the data points with a formula originally proposed by Sekoguchi et al (1982).

At relative low gas flow rates (U_G<40 m/s) and for all liquid rates tested, the film is highly asymmetric. As the gas flow rate increases, the liquid film height and the rest of its properties tend to be distributed uniformly around the pipe circumference, implying that the role of

gravity is almost negligible. Under these conditions, the similarity to vertical annular flow is striking.

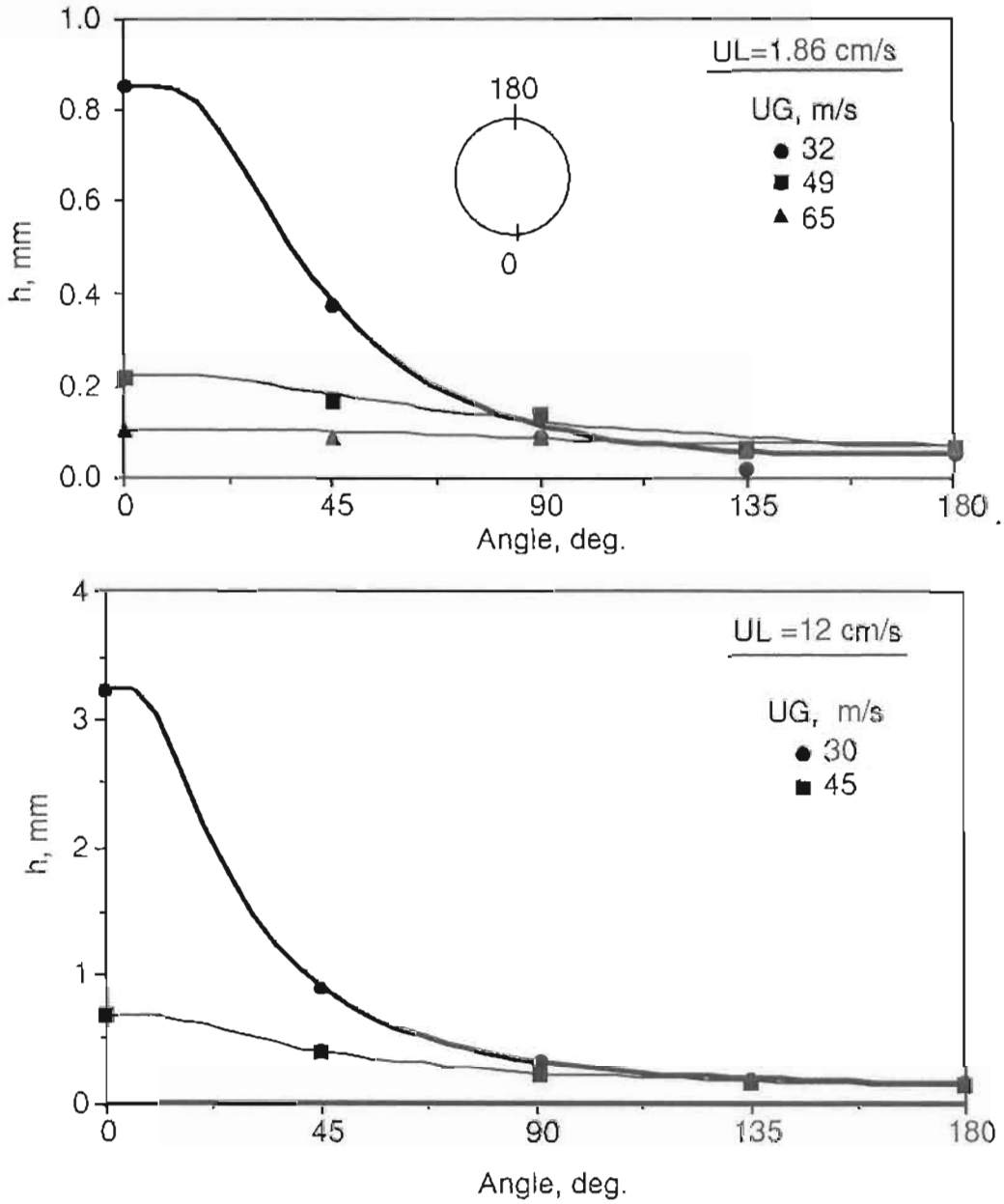

FIGURE 1. Film thickness distribution around the pipe circumference.

Typical RMS values of film thickness around the pipe circumference are presented in Figure 2, where solid lines are simply connecting the data points. RMS distribution exhibits the same behavior as the film thickness h.

The mean RMS value of the film thickness throughout the pipe cross-section, <RMS>, is calculated by integrating data, such as those of Figure 2, which cover one half of the pipe perimeter. This quantity could be useful in modeling various aspects of annular flow such as friction losses. An attempt to correlate the above mean RMS value with superficial liquid and gas velocities shows a strong influence of U_G and a weak influence of U_L, as follows

$$\langle RMS \rangle \quad U_L^{0.5}\, U_G^{-2.7}$$

The intensity of the film thickness fluctuations (Figure 3) is defined as **RMS/h**, where h and RMS are the local values of the time averaged film thickness and its standard deviation,

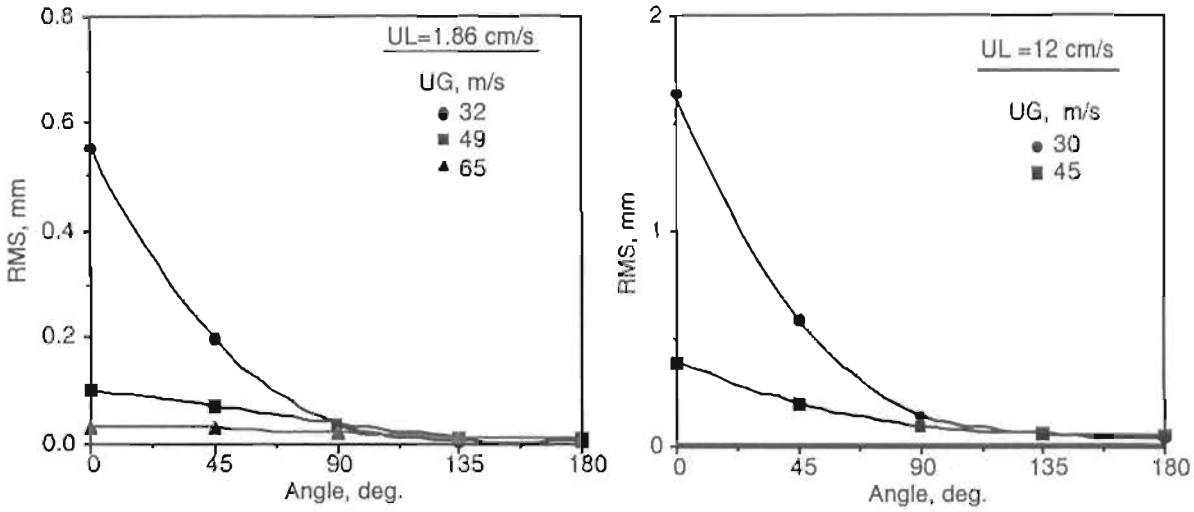

FIGURE 2. RMS values of film thickness around the pipe circumference.

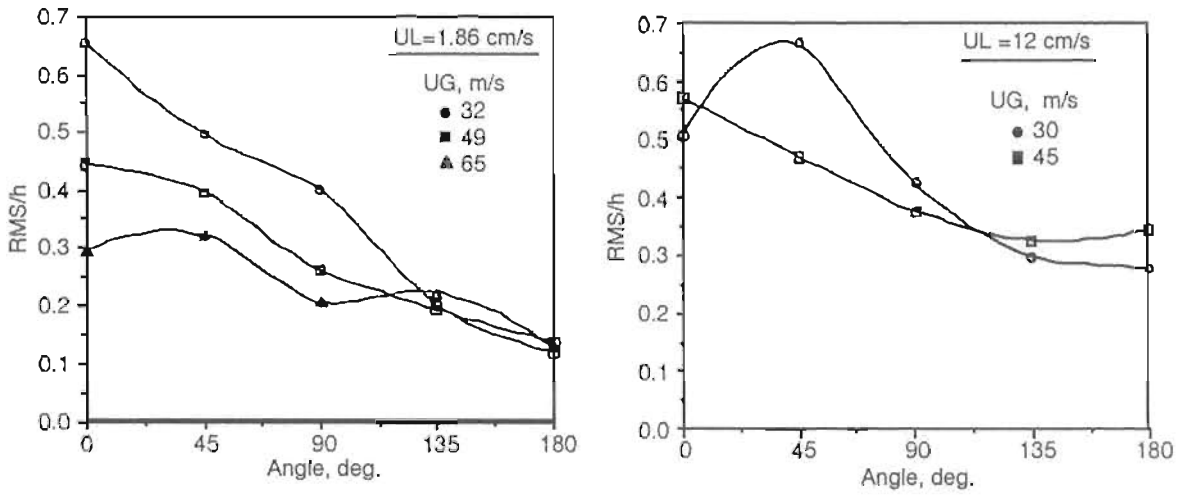

FIGURE 3. The intensity of the film thickness fluctuations.

respectively. At high gas flow rates the intensity of the film thickness fluctuations is almost symmetric around the pipe circumference, with a value of 0.2-0.3, whereas at low gas rates the distribution is highly asymmetric. Another interesting result is that, for low gas flow rates (30 m/s) and for U_L greater than 6 cm/s, the ratio RMS/h attains its maximum value at 45° rather than at 0°, where the maximum for all other cases is observed.

3.2 Wave Frequency and Celerity.

The power spectra of the film height time series have been obtained by averaging modified periodograms (Proakis and Manolakis, 1988). There is a 50% overlap between successive data segments each having 512 data points. The data are modified by a Parzen window before computing the periodogram. A 5-point smoothing procedure was employed on the final periodogram. According to Bendot and Piersol (1971) the resulting standard error on the final estimate is 11%, which is plotted as error bars on the power spectra.

Figure 4 shows that, for U_G< 35 m/s and for all liquid rates, a significant portion of the wave energy at the pipe bottom is carried by waves of frequency smaller than 10 Hz. An inspection of the film thickness traces and visual observations show that the dominant

frequencies of these spectra correspond to the characteristic frequencies of large disturbance waves. For higher gas flow rates and for U_L<12 cm/s a portion of the wave energy

is carried by waves of frequency greater than 15 Hz. The spectrum tends to flatten out drastically with increasing U_G, because energy is distributed uniformly among waves of higher frequencies and the liquid film thickness is also reduced (Paras and Karabelas, 1990).

Figure 5 shows typical power spectra of film thickness at three locations around the pipe circumference (0°, 45°, 90°) for the same flow conditions. The amplitude of the spectrum decreases by several orders of magnitude from the bottom of the pipe to an angular position of 90°. This trend is in accord with the circumferential variation of film thickness. No appreciable change of the dominant frequency can be detected in these spectra, especially at the lower part of the pipe. Moreover, it is noted that the frequency of large disturbance waves, defined as the peak frequency of the periodogram, tends to increase with U_G and to decrease with U_L.

The evidence presented so far (spectra, circumferential variation of h and RMS) clearly suggest that, at relatively low gas flow rates where gravity is important, the wave structure is dominated by the large disturbance waves at the pipe bottom.

Celerities of large waves are obtained by calculating the cross correlation function of two simultaneously recorded signals from locations at a distance Δx=6 cm and Θ=0Æ. The time delay ¢t, corresponding to the best correlation between the two signals, provides the celerity of such waves (Δx/¢t). Figure 6 indicates that disturbance wave celerity increases with increasing U_G and U_L.

Using light pulses of adjustable frequency, "ring-shaped" wave structures are observed to cover a large portion of the pipe circumference. For low U_G (less than 40 m/s) these ring-shaped waves move at an angle with respect to the pipe cross-section and with their front at the bottom. This angle is gradually reduced to zero with increasing gas flow rate. The visual observations are verified by calculating the time delay which corresponds to the best

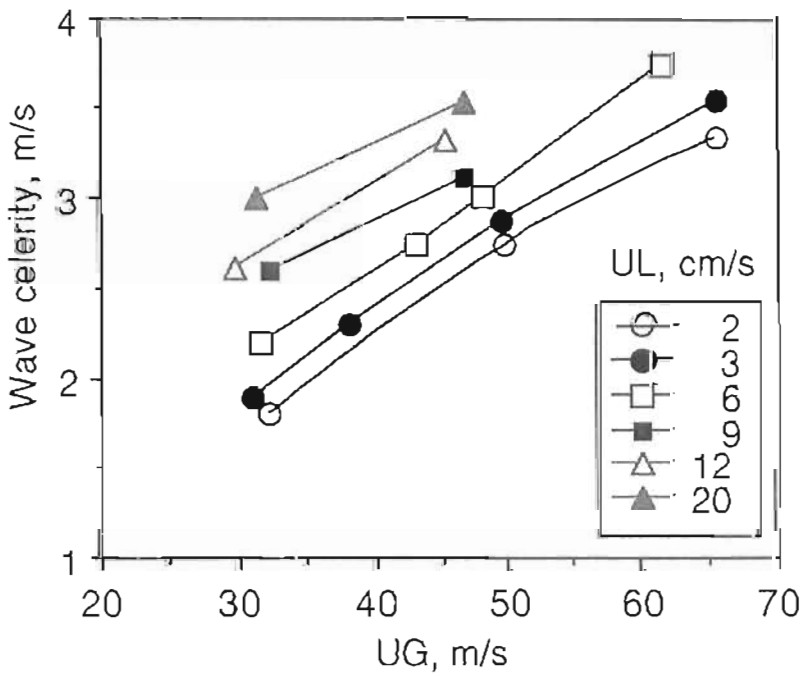

FIGURE 6. Large disturbance wave celerities.

correlation of the cross correlation function for the signals of two probes positioned at 0° and

TABLE 1. Time delay and the coefficient of correlation for two simultaneously recorded signals at $\Theta=0^o$ and $\Theta=90^o$.

U_L, m/s	U_G, m/s	Delay, ms	Correlation Coef.
0.02	32	28.0	0.211
0.02	66	1.0	0.192
0.06	32	6.0	0.451
0.06	62	0.2	0.204
0.09	33	13.0	0.595
0.09	47	0.5	0.367
0.12	30	7.0	0.648
0.12	45	4.0	0.354
0.20	32	9.0	0.388
0.20	47	1.0	0.360

90°, respectively. Table 1 presents the time delay and the coefficient of correlation between the two stations for various U_G and U_L. At low U_G and relatively high U_L values a better correlation is noticed between the two signals, suggesting a greater coherence of the ring-shaped structures.

3.3 Large Disturbance Wave Characteristics.

Wave intermittency, defined as the fraction of total sampling time corresponding to passage of large disturbance waves, is useful in the description of processes occurring at the gas/liquid interface (Schadel, 1988). This quantity is not easily extracted from the data, as it is difficult to unequivocally determine the amplitude of large disturbance waves. Nencini and Andreussi (1983) define the height difference between a minimum in the film trace and the subsequent maximum to be twice the wave amplitude. The large-wave height h_w is measured from the pipe surface.The wave width is the distance between two successive minima of the film trace, whereas the large-wave length is defined as the distance between the peaks of two such successive waves. Details on the procedure followed in calculating large disturbance-wave characteristics are presented elsewhere (Paras and Karabelas, 1990).

The mean large-wave height (h_w) at the bottom of the pipe ($\Theta=0^o$) computed with this procedure is found to be a linear function of the RMS value of the film height at $\Theta=0^o$ (Figure 7); i.e. $h_w = 4\ (RMS)_0$.

The strong influence of gas flow rate on the large-wave height is shown in Figure 8. The trend is similar to that for RMS values. The influence of superficial liquid velocity of the large-wave height is noticeable only at low gas flow rates; i.e., for $U_G < 50$ m/s. The mean large-wave width is well correlated with the corresponding large-wave length (Figure 9), being approximately 30% of the latter for all our experiments. This constant ratio is not surprising. Indeed, with increasing gas flow rate, the mean width tends to decrease and so does the mean length due to the increase of large wave frequency. The ratio of large-wave width to wave length essentially represents wave intermittency, which is almost independent of liquid and gas flow rates (Paras and Karabelas, 1990).

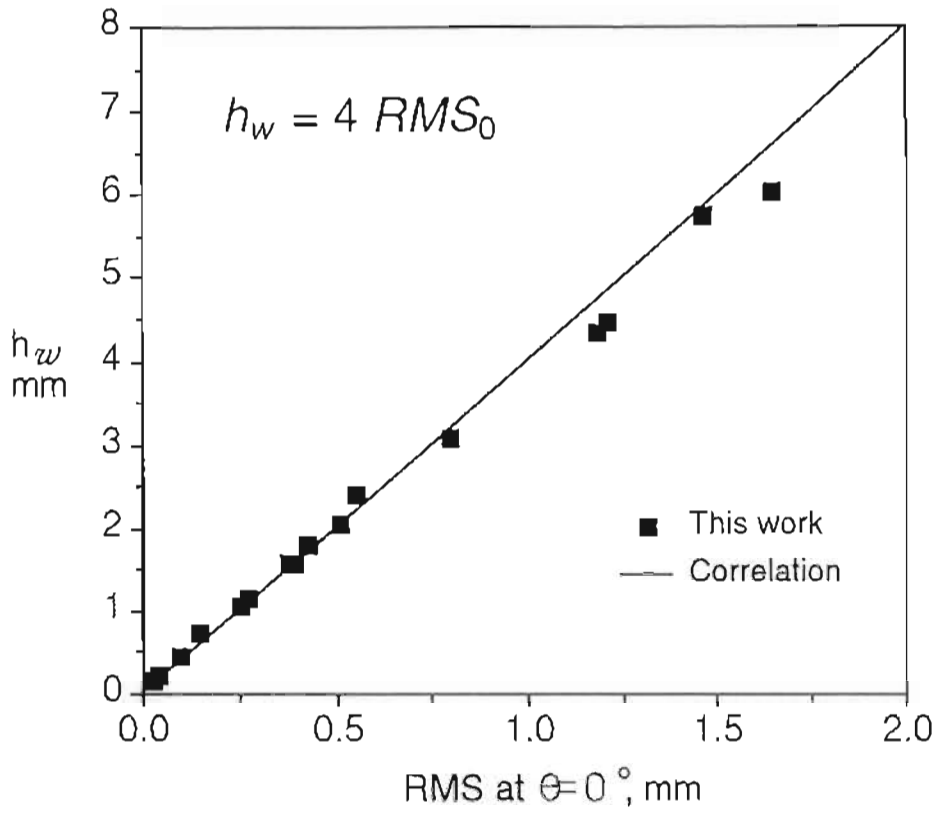

FIGURE 7. Mean height of large waves as a function of RMS at the pipe bottom, $\theta = 0^{o}$.

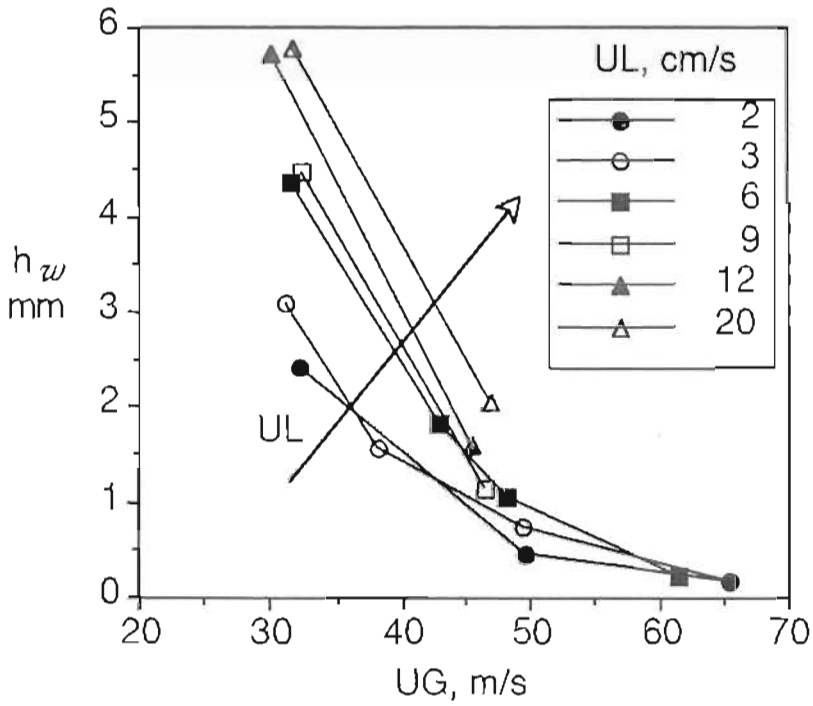

FIGURE 8. The influence of gas and liquid flow rate on the height of large waves, $\theta = 0^{o}$.

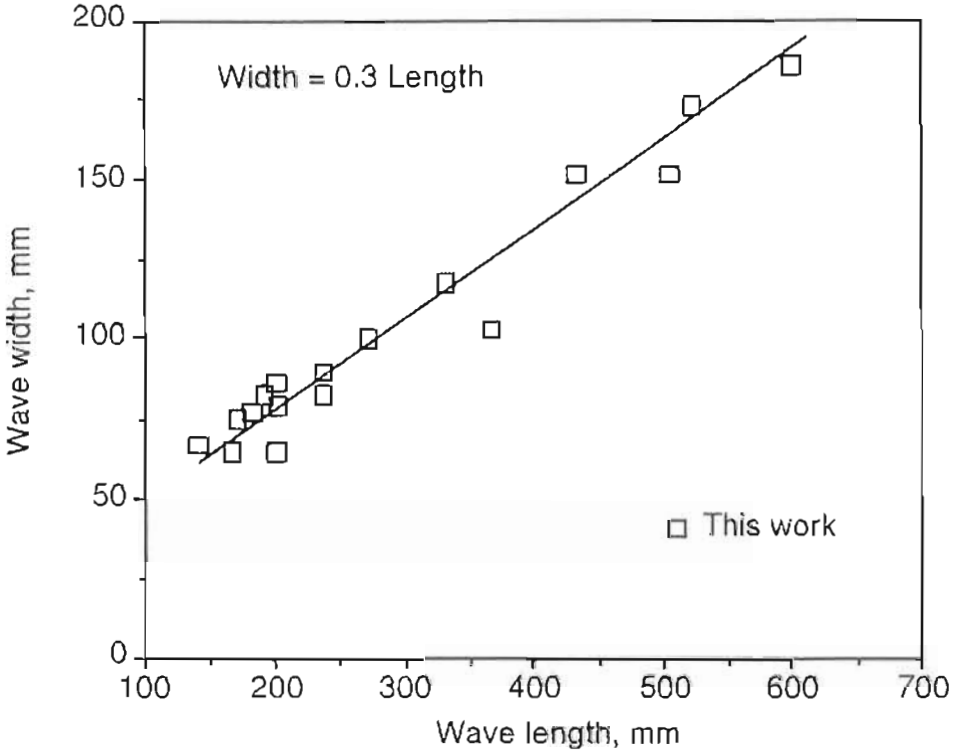

FIGURE 9. Correlation between the large disturbance wave width and length, $\theta=0^{o}$.

4. DISCUSSION

The data show the very strong effect of gas flow rate on the wave characteristics. At relatively small U_G, gravity plays an important role and a thick liquid layer is formed at the pipe bottom. Large disturbance waves are the dominant feature under these conditions. These large waves, of frequency smaller than 10 Hz, cover the lower part of pipe circumference at an angle with respect to the pipe cross-section. Moreover, for small U_G there are similarities between annular and stratified flow. With increasing gas flow rate, the large disturbance waves tend to cover a greater part of the circumference ("ring-shaped" waves) becoming more symmetrical and more frequent. At high gas velocities ($U_G > 50$ m/s) all the statistical quantities show that the flow tends to become axisymmetric and that the large waves gradually lose their significance.

Further interpretation of the statistical quantities obtained in this work is given elsewhere (Paras and Karabelas, 1990). Of particular interest appear to be wave intermittency, steepness and length, in connection with gas/liquid interface processes. Understanding these processes would be greatly aided by local velocity measurements in the film as well as in the gas phase. For this purpose, the use of Laser Doppler Anemometry is currently explored.

Acknowledgments. Financial support by the Commission of European Communities (Contract No EN3G-0040-GR) and the General Secretariat for Research & Technology of Greece is gratefully acknowledged.

5. REFERENCES

1. Andritsos, N., Effect of Pipe Diameter and Liquid Viscosity on Horizontal Stratified Flow, Ph.D. Thesis, University of Illinois, Urbana, 1986.

2. Bendat J.S. and A.G. Piersol, Random Data : Analysis and Measurement Procedures, Willey-Interscience, New York, 1971.

3. Karapantsios T.D., S.V. Paras and A.J.Karabelas, Statistical Characteristics of Free Falling Films at High Reynolds Numbers, *Int. J. Multiphase Flow*, vol. 15, no. 1, pp. 1-21, 1989.

4. Laurinat, J.E., Studies of the Effects of Pipe Size on Horizontal Annular Two-Phase Flows, Ph.D. Thesis, University of Illinois, Urbana, 1982.

5. Nencini, R.M. and P. Andreussi, Study of the Behavior of Large disturbance Waves in Annular Two-Phase Flow, *Can. J. Chem. Eng.*, vol. 60, pp. 459-466, 1983.

6. Paras S.V. and A.J.Karabelas, Properties of Liquid Layer in Horizontal Annular Flow, Submitted for publication, 1990.

7. Proakis, M. and Manolakis S., Introduction to Digital Signal Processing, MacMillan, 1988.

8. Schadel S.A., Atomization and Deposition Rates in Vertical Annular Two-Phase Flow, Ph.D. Thesis, University of Illinois, Urbana, 1988.

9. Sekoguchi K., A. Ousaka, T. Fukano and T. Morimoto, Air-Water Annular Two-Phase Flow in a Horizontal Tube, 1st Report, *Bulletin of the JSME*, vol. 25, p. 208, 1982.